JOURNAL OF AIRCRAFT
Vol. 40, No. 1, January–February 2003

Computer-Aided Assessment of Flight Simulator Fidelity

Y. Zeyada* and R. A. Hess†
University of California, Davis, California 95616-5294

A technique for computer-aided assessment of flight simulator fidelity is presented. The assessment procedure utilizes a mathematical model of the human pilot that includes proprioceptive, visual, and vestibular cues. The quality of the latter two cues can be varied to capture the effects of flight simulator limitations associated with visual and motion cueing. A MATLAB®-based tool that automates the selection of the majority of parameters in the pilot model and the generation of a fidelity metric is described. In addition, a prediction of the task-dependent handling qualities of the nominal flight vehicle can be obtained. The assessment procedure is exercised in a hypothetical example involving the six-degree-of-freedom control of a rotorcraft completing a vertical remask maneuver. It is demonstrated that by varying the quality of the visual and vestibular cues in the pilot/vehicle model the effects of simulator limitations upon fidelity can be systematically addressed.

Nomenclature

C	=	input to structural model of human pilot
$dvar$	=	variance of random number generator in visual cue model
$\boldsymbol{G}$	=	transfer function matrix defining inverse dynamic system
$\boldsymbol{G}_D$	=	transfer function matrix of inverted pilot/vehicle system
h_{com}, x_{com}, y_{com}, ψ_{com}	=	outer-loop commands in vertical remask maneuver, ft
h_{des}, x_{des}, y_{des}, ψ_{des}	=	desired time histories in vertical remask maneuver, ft
K_e	=	visual gain in structural model of human pilot
K_F	=	multiplying factor in half-power calculation of primary-loop crossover frequencies
$K_{\dot{m}}$	=	vestibular gain in structural model of human pilot
M	=	output of controlled element in structural pilot model
$p, \dot{\phi}$	=	roll rate, rad/s
$q, \dot{\theta}$	=	pitch rate, rad/s
$r, \dot{\psi}$	=	yaw rate, rad/s
ts	=	sampling period in zero-order hold element of visual cue model, s
U_M	=	proprioceptive feedback signal in structural pilot model
u	=	x body axis component of perturbation velocity, ft/s
v	=	y body axis component of perturbation velocity, ft/s
w	=	z body axis component of perturbation velocity, ft/s
Y_c	=	transfer function of controlled element in structural pilot model
Y_e	=	transfer function operating on visual error in structural pilot model, $K_e[(1 + (\varepsilon/s)]$
Y_{FS}	=	transfer function of force/feel system in rotorcraft cockpit
Y_{NM}	=	transfer function of neuromuscular system in structural pilot model
Y_{PF}	=	transfer model function of proprioceptive feedback system in structural pilot model
Yp_y, Yp_x, Yp_h, Yp_ψ	=	outer-loop pilot models for vertical remask maneuver
$Yp_{\dot{h}}$, Yp_θ, Yp_ϕ, $Yp_{\dot{\psi}}$	=	inner-loop pilot models for vertical remask maneuver, created by structural pilot model
δ_A	=	lateral cyclic input, inches of motion at pilot's hand (no SCAS case)
δ_{AP}	=	pilot's lateral cyclic cockpit input with SCAS, equivalent to roll attitude command, rad
δ_B	=	longitudinal cyclic input, inches of motion at pilot's hand (no SCAS case)
δ_{BP}	=	pilot's longitudinal cyclic input with SCAS, equivalent to pitch attitude command, rad
δ_C	=	main rotor collective input, inches of motion at pilot's hand
δ_P	=	tail rotor collective input, inches of motion at pilot's feet
ε	=	relative gain on integral error in Y_e
θ	=	vehicle pitch attitude, rad
τ_0	=	time delay in structural model of pilot, s
ϕ	=	vehicle roll attitude, rad
ψ	=	vehicle heading angle, rad
ω_{C_i}	=	estimated ith loop crossover frequency required in task being analyzed, rad/s

Received 19 June 2002; revision received 24 August 2002; accepted for publication 26 August 2002.

*Postdoctoral Researcher, Department of Mechanical and Aeronautical Engineering, One Shields Avenue; currently Assistant Professor, Faculty of Engineering, Cairo University, Giza, Egypt.

†Professor and Vice-Chairman, Department of Mechanical and Aeronautical Engineering, One Shields Avenue. Associate Fellow AIAA.

Introduction

HESS and Colleagues in Refs. 1–4 describe the evolution of an analytical technique for the assessment of flight simulator fidelity that employs pilot/vehicle analyses of aircraft as nominal flight vehicles and simulated versions of these vehicles. Analysis of the latter includes simulator limitations such as those introduced by motion system dynamics, simulator time delays, and, in the case of Ref. 4, degraded visual cues. The goals of the research to be described are 1) the extension of the work of Ref. 4 to analyses in which the pilot is controlling as many as four vehicle axes, 2) the creation of a MATLAB® and Simulink®-based assessment tool to support such a multiaxis pilot/vehicle analysis, and 3) the demonstration of this tool in assessing the fidelity of a hypothetical flight simulation of a realistic low-altitude rotorcraft maneuvering task incorporating a highly coupled vehicle model including stability and command augmentation systems.

The treatment begins with a description of the pilot model. This includes a definition of a handling qualities sensitivity function (HQSF), which forms the basis of the fidelity assessment technique.

An inverse dynamics formulation is included in this description that allows the compensatory pilot modeling procedure to produce realistic pilot/vehicle responses in discrete tracking tasks. The visual cue model is briefly reviewed. The fidelity assessment procedure is described next followed by a discussion of a computer-aided assessment tool MPVA (Multiaxis Pilot Vehicle Analysis). There follows an example in which MPVA is employed to analyze a hypothetical piloted simulation of a rotorcraft completing a vertical remask maneuver in which various flight simulator "limitations" are introduced. Conclusions are drawn to complete the presentation.

Model Description

Structural Pilot Model

The core of the methodology as presented in Ref. 4 is a structural pilot model.[5] Figure 1 shows this model for a single-axis task. This model is used to represent pilot control behavior in so-called "primary control loops," that is, those inner-control loops that involve direct pilot interaction with the cockpit inceptor. For example, a primary control loop might involve vehicle pitch attitude control with a control column or stick. This would be distinguished from an outer loop in which the pilot is using deviations from a desired altitude to command corrective pitch attitude changes. Such multiloop models are common in pilot/vehicle analyses.[6]

The pilot model shown in Fig. 1 can now be described in detail. $Y_e = K_e[1 + (\varepsilon/s)]$ is the pilot's visual proportional and low-frequency integral operation up on perceived error K_e is chosen to yield a desired inner-loop crossover frequency. τ_0 is 0.2 s.

$$Y_{\mathrm{NM}} = \frac{10^2}{s^2 + 2(0.707)10s + 10^2}$$

Y_{PF} is chosen as K, $K(s+a)$ or $K/(s+a)$ dependent upon the vehicle dynamics; one form is chosen so $Y_{\mathrm{PF}} \propto sY_c$ in the region of crossover. K is chosen so the minimum damping ratio of oscillatory poles of the closed-loop proprioceptive system is 0.15. K_m is chosen so that the minimum damping ratio of oscillatory poles of the closed-loop vestibular system is 0.05.

In Fig. 1 the HQSF is defined as

$$\mathrm{HQSF} = \frac{1}{K_e}\left|\frac{U_M}{C}(s)\right| \tag{1}$$

Hess[5,6] and Hess and Zeyada[7] demonstrate how the HQSF can be used to predict handling qualities levels and, in particular, Ref. 7 introduces the use of the HQSF to predict task-dependent handling qualities levels. As the name implies, task-dependent handling qualities are those that are dependent upon the particular task being performed by the pilot. Prediction of these handling qualities is pertinent to an assessment of the difficulty of the task being performed by the pilot of the nominal flight article and, in turn, by the pilot of the vehicle in the flight simulator.

Inverse Dynamics

Using a compensatory pilot model such as the structural model is attractive in pilot/vehicle analyses because these models and their

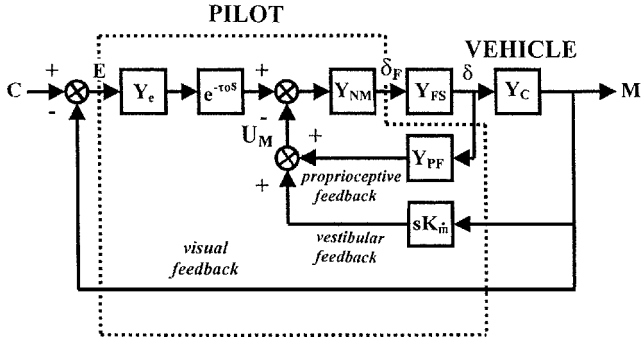

Fig. 1 Structural model of the human pilot.

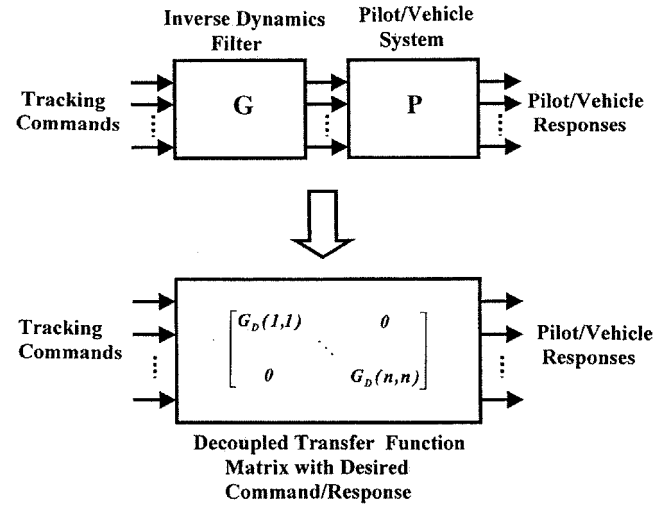

Fig. 2 Inverse dynamics system.

parameterization have been the subject of considerable research and validation over the past four decades. By "compensatory" we mean that the visual input to the pilot model is the error between the commanded and current value of a primary loop variable. With compensatory models the analyst can predict the basic form of pilot equalization given the dynamics of the vehicle and a hypothesized manual feedback topology.[6,8] A significant shortcoming in the use of compensatory pilot models arises in computer simulations of discrete maneuvers where unrealistic control activity and vehicle angular velocities are typically predicted at the maneuver initiation. By creating outer-loop command time histories that produce desired pilot/vehicle response time histories, one can eliminate the unrealistic vehicle responses just mentioned. This can be accomplished through inverse dynamic analysis. Figure 2 shows such an inverse dynamic system. The transfer function matrix $\boldsymbol{G}$ is created such that

$$\boldsymbol{P} \cdot \boldsymbol{G} = \boldsymbol{G}_D \approx \boldsymbol{I} \tag{2}$$

over a frequency range of interest for manual control ($0.1 < \omega < 10$ rad/s), where $\boldsymbol{I}$ is the identity matrix. The means for accomplishing this inversion is through the design of a linear dynamic inversion controller implemented as the matrix of transfer functions $\boldsymbol{G}$. Reference 4 describes creation of such controllers in detail. Thus, in a computer simulation of a pilot/vehicle system the tracking commands of Fig. 2 are desired outer-loop time histories. Often these desired time histories can be created by reference to the desired performance requirements of the maneuver itself, for example, as provided in the rotorcraft low-speed maneuver descriptions in Ref. 9. This will be demonstrated in the example of the vertical remask maneuver to be discussed.

Visual Cue Model

The visual cue model is an important element in the complete pilot model formulation. The model itself is shown in Fig. 3 and described in detail in Ref. 4. In the model each visually derived signal that the pilot is assumed to use is fed through a sample and hold element, with the sampling period denoted as *ts*. Referring to Fig. 1, and assuming a single-axis laboratory tracking task is being considered in which the error signal E is the only displayed signal, the model of Fig. 3 would be inserted immediately before the element Y_e. As Fig. 3 indicates, the resulting discrete signal is multiplied by a magnitude-limited random number, with variance *dvar*, and is then filtered. The resulting filtered signal is added to the output of the sample and hold element to produce the visual cue model output.

The noise input of the model of Fig. 3 is multiplicative in nature. Hess and Siwakosit[4] showed that by creating an effective remnant signal injected in parallel with the visual input in a simulated single-axis tracking task the visual cue model of Fig. 3 reproduced two

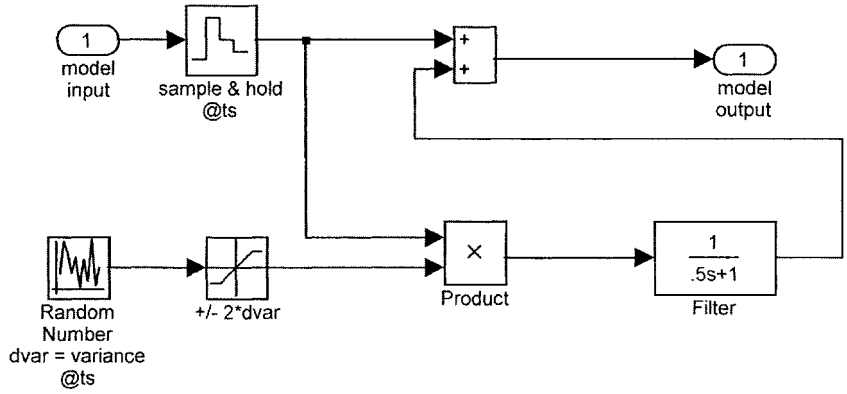

Fig. 3 Visual cue model.

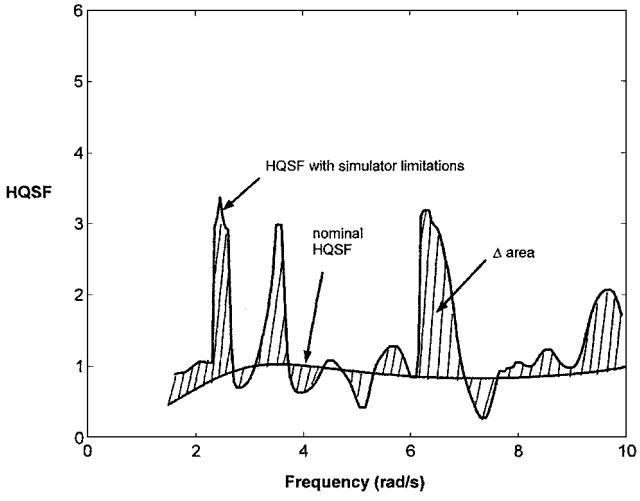

Fig. 4 Example of Δarea calculation in fidelity metric.

important characteristics of modeled human pilot remnant signals. These characteristics are 1) a first-order power spectral density with 2) an intensity that scaled with the variance of the error signal to which it was added.[10] The parameter *dvar* was also shown to play a role similar to the noise-signal ratio of injected observation noise in algorithmic models of the human pilot such as the Optimal Control Model (OCM).[6]

Fidelity Assessment Procedure

In the fidelity assessment procedure to be demonstrated, a pilot/vehicle structure is created for the nominal flight vehicle. This can include pilot models in both primary and outer loops. The resulting model is then frozen, and various simulator limitations are introduced. The behavior of the pilot model tuned to the nominal vehicle but controlling the simulated vehicle is used to assess the impact of the limitations upon simulator fidelity. The HQSFs derived for the nominal and simulated vehicle form the basis of the fidelity assessment. Figure 4 shows two HQSFs: one for a nominal vehicle and one for the vehicle with simulator limitations. The area between the curves is calculated as Δarea. This area is then normalized by dividing by a normalizing area, that is, the area beneath the HQSF curve for the nominal vehicle. The resulting number, referred to as a "fidelity metric," was shown in Ref. 4 to predict fidelity degradations consistent with those reported in the literature.[11–13] For multiaxis applications the fidelity metric becomes

$$\text{fidelity metric} = \frac{1}{n}\sum_{i=1}^{n}\left[\frac{\Delta\text{area}}{\text{normalzing area}}\right]_i \qquad (3)$$

where n is the total number of inner-loop axes being controlled by the pilot. The larger the value of the metric in Eq. (3), the poorer is the predicted simulator fidelity.

Computer-Aided Assessment

Creation of the structural pilot models, the inverse dynamics system, and calculation of the fidelity metric for a simulator fidelity assessment can be quite time consuming. To this end, a MATLAB and Simulink-based tool has been created, referred to as MPVA.[14] This assessment tool 1) automates the selection of the majority of the structural pilot model parameters, 2) creates the inverse dynamics system, 3) calculates the required crossover frequencies for the estimation of task-dependent handling qualities, 4) calculates the fidelity metric of Eq. (3) when the pilot/vehicle system is simulated in Simulink, and 5) provides a prediction of the task-dependent handling qualities of the nominal vehicle in the maneuver in question.

MPVA employs a graphical-user interface (GUI) that simplifies the creation and evaluation of a multiaxis pilot/vehicle system. In MPVA the user begins with a linear, state-space description of the vehicle, including any stability augmentation systems that might be employed. Next, through the GUI the user creates the structural models for each "primary" control loop assuming nominal 2.0 rad/s primary control loop crossover frequencies. Following this, a computer simulation of the pilot/vehicle system is created in Simulink. This step is the most time-consuming aspect of the procedure and involves building the models for the motion system dynamics and implementing the various feedback paths for the visual and vestibular signals to serve as inputs to structural pilot model and any outer-loop pilot models that are required.

After the Simulink model is complete, MPVA will compute the inverse dynamics model for the nominal system by invoking a MATLAB m-file. Next, the desired vehicle response time histories are created and implemented by the user. Once this is accomplished, the computer simulation is repeated using the desired time histories as inputs to the inverse dynamics system $\boldsymbol{G}$. Next, another m-file is invoked, which calculates and implements the task-dependent crossover frequencies, and a new inverse dynamics system $\boldsymbol{G}$ is created corresponding to these modified crossover frequencies. With these crossover frequencies and new $\boldsymbol{G}$ in place, the user calculates the nominal HQSFs, then introduces the various flight simulator limitations. With the latter in place, the Simulink simulation is repeated, and MPVA calculates the fidelity metric given by Eq. (3).

Fidelity Assessment Example

Performance Requirements

An example of analytical simulator fidelity assessment will be presented involving a BO-105 rotorcraft completing a vertical remask maneuver, which is described in Ref. 9. The flight simulator limitations will include the three sets of motion system dynamics: 1) fixed base (no motion), 2) moving base dynamics approximating those of a hexipod system, and 3) moving base dynamics approximating those of a large-motion flight simulator such as the NASA-Ames Vertical Motion Simulator (VMS). In addition, the visual cue model discussed in a preceding section will be employed to model limitations in visual scene representation in a flight simulator.

The vehicle dynamics were taken from Ref. 15. The BO-105 model was chosen because of the significant longitudinal–lateral

dynamic coupling that exists attributable to the soft in-plane hingeless rotor. Data for the hover flight condition were chosen. The unaugmented vehicle model is given here:

$$\begin{Bmatrix} \dot{u} \\ \dot{w} \\ \dot{q} \\ \dot{v} \\ \dot{p} \\ \dot{r} \\ \dot{\theta} \\ \dot{\phi} \\ \dot{\psi} \end{Bmatrix} = \begin{bmatrix} -0.01660 & 0.01241 & 1.6150 & 0.00040 & -0.7260 & -0.11920 & -32.17 & 0 & 0 \\ 0.01 & -0.3317 & 0.33 & -0.001 & 0.1473 & 1.8309 & 0 & 0 & 0 \\ 0.0202 & -0.0027 & -3.3972 & -0.004 & -0.84 & 0.0439 & 0 & 0 & 0 \\ -0.0012 & -0.0054 & -0.4834 & -0.032 & -1.7454 & 0.205 & 0 & 32.17 & 0 \\ -0.0111 & -0.0121 & 2.3 & -0.632 & -9.244 & -0.224 & 0 & 0 & 0 \\ -0.0008 & 0.0018 & -0.1215 & 0.0099 & -0.0759 & -0.327 & 0 & 0 & 0 \\ 0 & 0 & 1 & 0 & 0 & 0 & 0 & 0 & 0 \\ 0 & 0 & 0 & 0 & 1 & 0 & 0 & 0 & 0 \\ 0 & 0 & 0 & 0 & 0 & 1 & 0 & 0 & 0 \end{bmatrix} \begin{Bmatrix} u \\ w \\ q \\ v \\ p \\ r \\ \theta \\ \phi \\ \psi \end{Bmatrix}$$

$$+ \begin{bmatrix} 0.4467 & 0.7894 & -0.0045 & -0.12 \\ -9.881 & 0.0429 & -0.016 & -0.0131 \\ -0.0805 & -0.9727 & 0.1598 & 0.0577 \\ -0.0489 & 0.0383 & 0.8014 & -1.6381 \\ -0.1275 & 0.459 & 2.644 & -1.0126 \\ 0.5651 & -0.0045 & 0.0341 & 1.3931 \\ 0 & 0 & 0 & 0 \\ 0 & 0 & 0 & 0 \\ 0 & 0 & 0 & 0 \end{bmatrix} \begin{Bmatrix} \delta_C \\ \delta_B \\ \delta_A \\ \delta_P \end{Bmatrix}$$

Although the vertical remask maneuver will involve lateral velocities that are beyond those accurately modeled by hover dynamics, the hover flight condition was retained for simplicity. The bare-airframe dynamics in pitch and roll were augmented by the attitude-hold/attitude-command stability and command augmentation systems (SCAS) given here:

Pitch-attitude loop:

$$\frac{\delta_B}{(\delta_{\mathrm{BP}} - \theta)} = -\frac{100(1)(4)^2}{(0)^2(20)}$$

where the socond half of the equation is equal to $-[100(s+1)(s+4)^2/s^2(s+20)]$

roll-attitude loop:

$$\frac{\delta_A}{(\delta_{\mathrm{AP}} - \phi)} = \frac{100(1)(4)^2}{(0)^2(20)}$$

The bandwidths of these SCAS systems were approximately 4 rad/s and were included in the example to provide a realistic model for evaluation. Thus the complete, augmented vehicle model contains 15 states and four control inputs, a significant increase in complexity over the simple four-state, two-input model of Ref. 4.

The vertical remask maneuver is described in Ref. 9 as follows: "From a stabilized hover at 75 ft, remask vertically to an altitude below 25 ft. Then rapidly displace the rotorcraft laterally 300 ft and stabilize at a new hover position." Table 1 shows the desired performance for this maneuver. Based upon this description and a safety of flight limitation of maintaining realistic vehicle roll attitude excursions ($\phi_{\max} \cong \pm 40$ deg), the $h_{\mathrm{des}}(t)$ and $y_{\mathrm{des}}(t)$ time histories were created. Note that $x_{\mathrm{des}}(t)$ and $\psi_{\mathrm{des}}(t)$ are both zero. These time histories are shown in Fig. 5 along with the scaled time history of the vehicle roll attitude that resulted in the Simulink simulation of the pilot/vehicle system.

Assumed Pilot Loop Closures

Figure 6 shows the assumed pilot loop closures for the analysis. Note that the block labeled "vehicle+ SCAS" contains the attitude SCAS for the pitch and roll loops. The primary loops are seen to include control of heave rate, pitch attitude, roll attitude, and yaw rate. Outer-loop pilot closures are also in evidence, consisting of simple gains for the heave and yaw loops, and low-frequency lead for the x- and y-displacement loops. The initial crossover frequencies of the pilot modeling procedure were 2 rad/s for the primary loops and 1 rad/s for the outer loops. As will be seen, these initial crossover frequencies will be modified to reflect task-dependent handling qualities. Table 2 shows the pilot model parameters for

Table 1 Performance requirements from Ref. 9—Vertical remask maneuver

Performance	Desired	Adequate
Achieve an altitude of X or less within 6 s of initiating the maneuver	25 ft	NA
During initial stabilized hover, vertical descent, and final stabilized hover, maintain longitudinal and lateral position within $\pm X$ ft of a reference point on ground	8 ft	12 ft
Maintain altitude after remask and during displacement within X ft	10 ft	+10 and −15 ft
Maintain heading within $\pm X$ deg	10 deg	15 deg
Maintain lateral ground track within $\pm X$ ft	10 ft	15 ft
Achieve a stabilized hover within X s after reaching final hover position	5 s	10 s
Achieve a final stabilized hover within X s of initiating the maneuver	15 s	25 s

Table 2 Pilot model parameters[a]

Primary-loop feedback variable	Structural pilot model parameters (primary control loops) Y_{PF}	Y_{FS}	Y_e	$K_{\dot{m}}$
$\dot{h}$	$\frac{9.36}{(4.5)}$	$\frac{10}{(10)}$	$\frac{0.985(.5)}{(0)}$	0.183
θ	0.24(0.5)	$\frac{25^2}{[0.7, 25]}$	1.9	0.322
ϕ	0.216(0.5)	$\frac{25^2}{[0.7, 25]}$	2.03	0.125
$\dot{\psi}$	$\frac{8.16}{(4.5)}$	$\frac{25^2}{[0.7, 25]}$	$\frac{5.57(0.4)}{(0)}$	1.081

[a]Parameters correspond to primary- and outer-loop crossover frequencies of 2.0 and 1.0 rad/s, respectively.

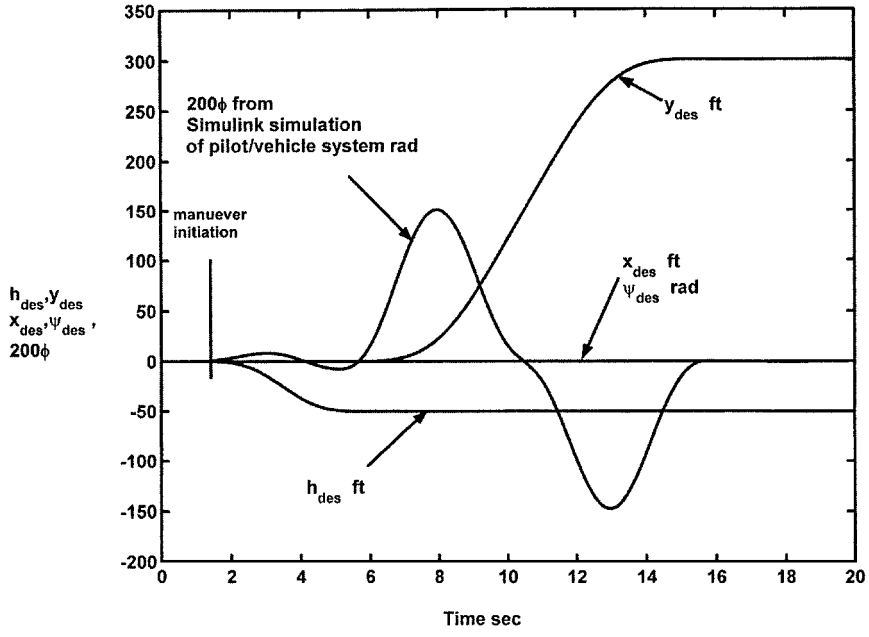

Fig. 5 Desired pilot/vehicle time histories for verticle remask maneuver and scaled roll attitude excursions that result.

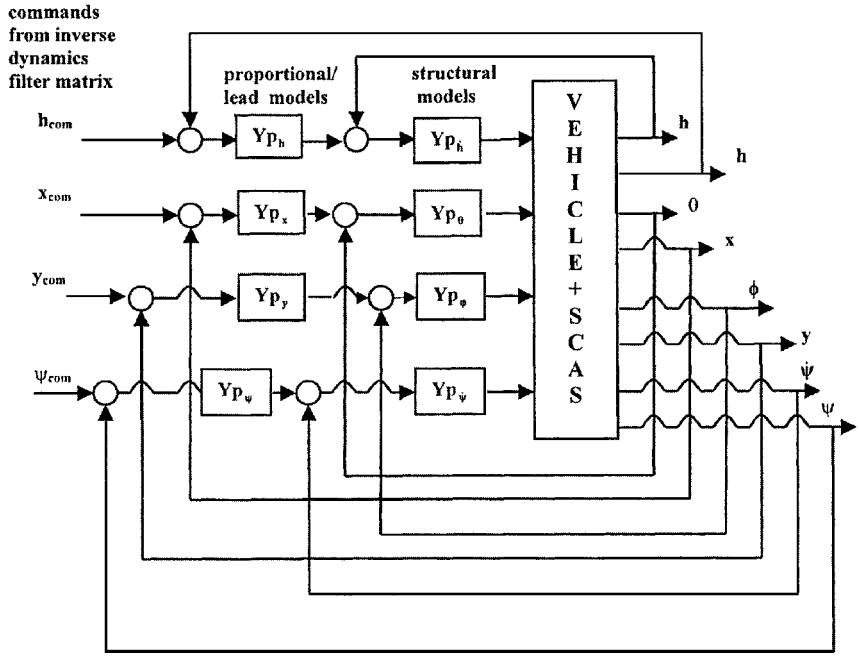

Fig. 6 Hypothesized pilot loop closures for verticle remask maneuver.

the inner and outer loops of Fig. 6. The outer-loop pilot models are $Y_{p_h} = 0.89$, $Y_{p_x} = -0.037(0.1)$, $Y_{p_\psi} = 0.037(0.1)$, and $Y_{p_\psi} = 0.89$.

Simulator Motion Dynamics

Table 3 lists the assumed dynamics of the simulator motion systems. In addition to those listed, of course, a fixed-base (no motion) simulator will be considered. The motion dynamics are identical to those employed in Ref. 4. In addition, as was done in Ref. 4, it was hypothesized that outer-loop motion quantities such a longitudinal and lateral acceleration [$\ddot{x}(t)$ and $\ddot{y}(t)$] could serve as surrogate cues for pitch and roll attitude $\theta(t)$ and $\phi(t)$. Thus the visual workload in the pitch and roll attitude tasks could be lessened. The surrogate cues were blended with the visually sensed attitude cues as follows:

$$\theta_{\text{sensed}}(t) = 0.75\theta_{\text{visual}}(t) - \frac{0.25}{32.2}\ddot{x}(t)$$

$$\phi_{\text{sensed}}(t) = 0.75\phi_{\text{visual}}(t) + \frac{0.25}{32.2}\ddot{y}(t) \qquad (4)$$

The assumption of a 75/25 gain distribution between the visual and proprioceptive signals is somewhat arbitrary; however, the impact of this assumption on fidelity assessment is mitigated by the fact that the gain values remain invariant in the analysis.

Visual Cue Model

Visual cue models such as that of Fig. 3 were implemented in the feedback path of each visually sensed variable in the system of Fig. 6, for example, in the $\dot{h}$ and h feedback paths. In addition, to account for the fact that internally generated command signals created by the pilot must be interpreted in the visual field, visual cue models were implemented in the forward path before and after each outer-loop pilot compensation element, for example, Yp_h in Fig. 6. In creating an outer-loop compensation such as Yp_x, if a lead term is required, that is, if Yp_x is given by

$$\theta_c = Yp_x x_e = K_x(T_{\text{Lx}}s + 1)x_e$$

$$= K_x T_{\text{Lx}}(\dot{x}_{\text{com}} - \dot{x}) + K_x(x_{\text{com}} - x) \qquad (5)$$

Table 3 Simulator motion system dynamics

Axis	Small motion	Large motion
Heave	$\frac{0.13(0)^2}{[0.707, 0.9]}$	$\frac{0.8(0)^2}{[0.707, 0.3]}$
Pitch	$\frac{0.25(0)}{(0.81)}$	$\frac{0.4(0)^2}{[0.707, 0.5]}$
Roll	$\frac{0.25(0)}{(0.81)}$	$\frac{0.4(0)^2}{[0.707, 0.5]}$
Yaw	$\frac{0.25(0)}{(0.81)}$	$\frac{0.4(0)^2}{[0.707, 0.5]}$

then separate visual cue models were included for the rate terms and the displacement terms. This formulation leads to 14 separate visual cue models in the Simulink implementation of the pilot/vehicle system, again a considerable increase in complexity over the model of the pilot/vehicle system in Ref. 4. It is useful to place the number of visual cue models required in this analysis in context. A pertinent comparison can be made between the pilot/vehicle model used here and the OCM of the human pilot.[6] The OCM has been used by the second author in a pilot/vehicle analysis of a rotorcraft in a landing approach task.[16] In Ref. 16 the pilot was required to control the same number of axes as that employed in the present example. The resulting OCM required 16 separate visual channels in which observation noise was injected in parallel with visually sensed inputs to model the human visual processing system. In this light the 14 visual cue models employed in the present example are reasonable.

Results

The modified primary-loop crossover frequencies for the heave rate, pitch attitude, roll attitude, and yaw rate loops were determined to be 1.66, 1.87, 0.96, and 0.75 rad/s, respectively. The outer-loop crossover frequencies were modified to retain the factor of two separation. The values just cited represent estimates of the primary-loop crossover frequencies required in the task being analyzed. They are obtained from MPVA as follows: A computer simulation of the pilot/vehicle system in the vertical remask maneuver is conducted, with the 2.0 and 1.0 rad/s primary- and outer-loop crossover frequencies in evidence. The required crossover frequency ω_{C_i} for the ith loop is estimated from

$$0.5 = \frac{\int_0^{\omega_{C_i}/K_F} \Phi_{\delta_i\delta_i}(\omega)\,\mathrm{d}\omega}{\int_0^{\infty} \Phi_{\delta_i\delta_i}(\omega)\,\mathrm{d}\omega} \tag{6}$$

With $K_F = 1$ the ω_{C_i} of Eq. (6) would correspond to the half-power frequency in the pilot's control output δ_i. Here $K_F = 1.35$. This larger value produced ω_{C_i} values that more closely approximated those obtained by the procedure in Ref. 7, that is,

$$\omega_{C_i} = 2.4\frac{\dot{x}_i|_{\max}}{x_i|_{\max}} \tag{7}$$

Here, x_i represents the primary-loop vehicle-response variable in the ith loop. Equation (7) cannot be employed in multiaxis tasks where $x_{i_{\text{desired}}} = 0$; hence, Eq. (6) is utilized. The new primary- and outer-loop crossover frequencies are implemented, and a new inverse dynamic matrix $\boldsymbol{G}$ is obtained. This $\boldsymbol{G}$ is used to obtain the HQSFs.

Each HQSF is calculated with the remaining loops closed. Thus, each HQSF includes the effects of pilot model activity in all other axes. With this in mind, the following supposition can be made: The overall handling qualities prediction for a task will be determined by the poorest predicted handling qualities level for any axis. Obviously this is something of an assertion at this point; however, research that has been directed toward determining multiaxis handling qualities ratings is quite sparse.[17,18] The HQSF results indicate violations of the level 1 boundary for all but the pitch attitude loop. Thus level 2 handling qualities are predicted. Figure 7 shows the HQSF for the heave rate loop that exhibited the most significant level 1

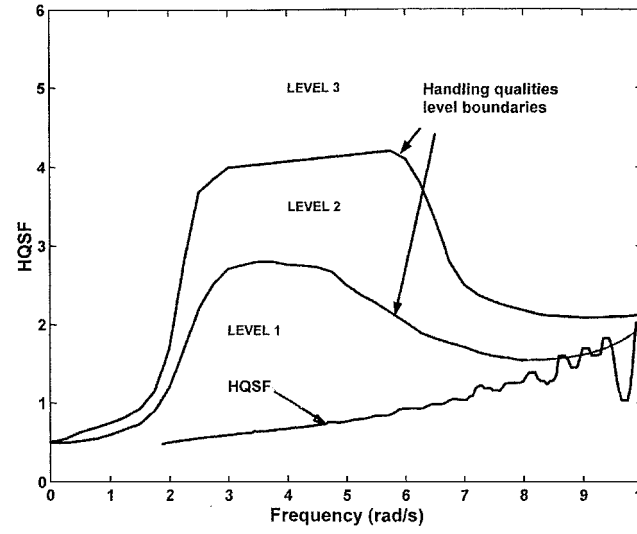

Fig. 7 HQSF for heave rate loop indicating level 2 task-dependent handling qualities.

boundary violation of the pilot/vehicle system. The prediction of handling qualities levels as developed in Ref. 5 requires only a single violation of any bound to move from one level to the next. So, for example, the relatively minor violation of the level 1 bound in Fig. 7 is sufficient to yield a prediction of level 2 handling qualities for that axis. Figure 8 shows the pilot model control inputs for the maneuver with the modified crossover frequencies given at the beginning of this section. Note the significant coupling that occurs during the maneuver.

The following combination of simulator characteristics was evaluated with in the vertical remask maneuver of Table 1.

Sim0: Perfect motion, no visual cue degradation (nominal flight vehicle)

Sim1: No motion, no visual cue degradation

Sim2: Small motion, no visual cue degradation

Sim3: Large motion, no visual cue degradation

Sim4: Large motion, visual cue degradation with $dvar = 0.1$ and $ts = 0.06$ s

Sim5: Perfect motion, visual cue degradation with $dvar = 0.1$ and $ts = 0.06$ s

Sim6: Large motion, visual cue degradation with $dvar = 0.1$ and $ts = 0.06$-s and 0.05-s delay in visual scene and motion system dynamics

The values of $dvar$ and ts are identical to the values used in Ref. 4. With $dvar = 0.1$ the largest multiplicative error occurring in the visual channel at any time would be 20% [recall the saturation element with limits of $\pm 2(dvar)$ in the visual cue model]. The sampling period of the zero-order hold in the visual cue model was chosen to provide a sampling frequency approximately 50 times the closed-loop pilot/vehicle bandwidth when crossover frequencies of 2 rad/s were employed.

Table 4 lists the values of the fidelity metric with each of the systems above. Note that the nominal flight vehicle receives a metric value of zero. Although limited in terms of the number of combinations of simulator limitations that have been introduced, the results summarized in Table 4 exemplify one way in which the fidelity assessment tool that has been described can be used. Namely an analysis of the sensitivity of a particular vehicle and task simulation to variations in simulation parameters can be undertaken. Here, for example, changing from the small motion (hexapod-like) to the large motion (VMS-like) systems produces a significant increase in fidelity (decrease in metric value), even when visual cue degradation is included in the latter. Likewise, elimination of motion cues implies serious fidelity issues for this particular vehicle and task resulting, as it does, in the largest fidelity metric (poorest fidelity).

The infinite value of the no-motion case indicates that the pilot/vehicle system was unstable as simulated here in MPVA. It must be emphasized that this does not imply that a fixed-base

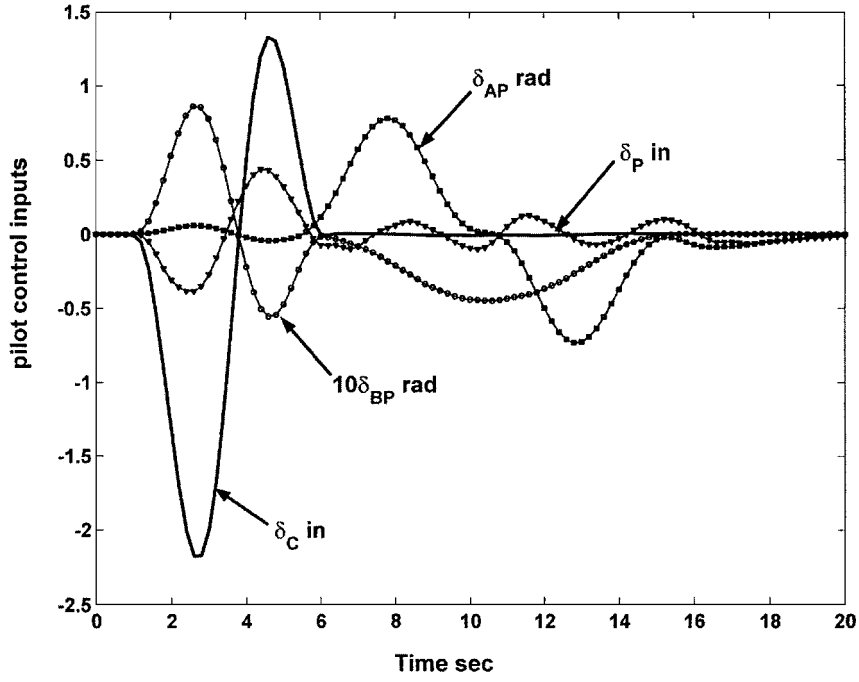

Fig. 8 Pilot model inputs for vertical remask maneuver with task-dependent crossover frequencies.

Table 4 Fidelity metric values

Simulation definition	Value of fidelity metric
Sim0 Perfect motion, no visual cue degradation (nominal flight vehicle)	0
Sim1 No motion, no visual cue degradation	∞[a]
Sim2 small motion, no visual cue degradation	3.71
Sim3 large motion, no visual cue degradation	0.34
Sim4 large motion, visual cue degradation $dvar = 0.1$; $ts = 0.06$ s	2.07
Sim5 perfect motion, visual cue degradation $dvar = 0.1$; $ts = 0.06$ s	1.51
Sim6 Large motion, visual cue degradation $dvar = 0.1$; $ts = 0.06$ s; 0.05-s delay in visual scene and motion system dynamics	2.16

[a]Pilot/vehicle system unstable.

pilot-in-the-loop simulation of this system would, in reality, be unstable, rather that the closed-loop system is unstable when "flown" with pilot model parameters tuned to the nominal flight vehicle with no simulator limitations. The no-motion case is worthy of further comment. Reference 19 presents the results of a pilot-in-the-loop simulator fidelity study involving a simple rotorcraft model being controlled in the vertical and directional axes in the NASA VMS. The similarity in the vertical task studied in Ref. 19 and the vertical portion of the vertical remask studied here invites comparison. One of the conclusions of Ref. 19 states:

> Pilots were surprised at the performance results and how their technique had to change when all motion was removed. Two of the three pilots input collective displacements *in the wrong direction* when flying fixed base [emphasis added]. Until the value of motion was demonstrated, pilot subjective impression was that the vertical axis was primarily visual. Thus, caution should be used when interpreting piloted subjective impression of the value of motion.

The fact that the pilots of Ref. 19 had to change their control technique in the absence of motion is, according to our philosophy, prima facie evidence of serious fidelity issues. However, the question of whether this adaptation is harmful for either training or engineering-system-development can be debated.

Two important issues remain in the fidelity assessment technique just described and exercised. These relate to means of correlating the value of the fidelity metric with subjective measures of simulator fidelity and a means of correlating a given visual scene representation in a flight simulation with specific value of the parameters *dvar* and *ts*. Research in this area is being pursued.

Conclusions

A computer-aided technique can be employed to analyze the effects of flight simulator limitations upon flight simulator fidelity. As demonstrated with a realistic, six-degree-of-freedom computer simulation of a rotorcraft completing a vertical remask maneuver, the MATLAB-based assessment procedure builds upon well-established models for the human pilot and automates many of the calculations involved in creating and implementing these models. The resulting pilot models utilize the three major cues employed in human vehicular control: proprioceptive, visual, and vestibular. In addition to providing a fidelity metric for any flight simulation exercise, the tool also predicts the task-dependent handling qualities of the nominal flight article in the maneuver being simulated. Although much of the pilot/vehicle analysis is automated, significant effort is still involved in creating the computer simulation of the complete pilot/vehicle system.

Acknowledgment

This work was supported by a Cooperative Research Agreement with NASA Ames Research Center. The grant technical manager was Duc Tran.

References

[1]Hess, R. A., and Malsbury, R., "Closed-Loop Assessment of Flight Simulator Fidelity," *Journal of Guidance, Control, and Dynamics*, Vol. 14, No. 1, 1991, pp. 191–197.

[2]Hess, R. A., Malsbury, T., and Atencio, A., Jr., "Flight Simulator Fidelity Assessment in a Rotorcraft Lateral Translation Maneuver," *Journal of Guidance, Control, and Dynamics*, Vol. 16, No. 1, 1993, pp. 191–197.

[3]Zeyada, Y., and Hess, R. A., "Human Pilot Cue Utilization with Applications to Simulator Fidelity Assessment," *Journal of Aircraft*, Vol. 37, No. 4, 2000, pp. 588–597.

[4]Hess, R. A., and Siwakosit, W., "Assessment of Flight Simulator Fidelity Including Visual Cue Quality," *Journal of Aircraft*, Vol. 38, No. 4, 2000, pp. 607–614.

[5]Hess, R. A., "A Unified Theory for Aircraft Handling Qualities and Adverse Aircraft-Pilot Coupling," *Journal of Guidance, Control, and Dynamics*, Vol. 20, No. 6, 1997, pp. 1141–1148.

[6]Hess, R. A., "Feedback Control Models—Manual Control and Tracking," *Handbook of Human Factors and Ergonomics*, 2nd Ed., edited by G. Salvendy, Wiley, New York, 1997, Chap. 38, pp. 1249–1294.

[7]Hess, R. A., and Zeyada, Y., "Modeling and Simulation for Helicopter Task Analysis," *Journal of the American Helicopter Society*, Vol. 47, No. 4, 2002, pp. 243–252.

[8]McRuer, D. T., and Krendel, E. S., "Mathematical Models of Human Pilot Behavior," AGARDograph 188, 1974.

[9]"ADS-33E-PRF, Aeronautical Design Standard, Performance Specification, Handling Qualities Design Requirements for Military Rotorcraft," U.S. Army Aviation and Missile Command, Redstone Arsenal, AL, March 2000.

[10]Jex, R., Allen, R. W., and Magdaleno, R. E., "Display Format Effects on Precision Tracking Performance, Describing Functions, and Remnant," Aerospace Medical Research Lab., AMRL-TR-71-63, Wright–Patterson AFB, OH, Aug. 1971.

[11]Schroeder, J. A., Chung, W. W. Y., and Hess, R. A., "Evaluation of Motion Fidelity Criterion with Visual Scene Changes," *Journal of Aircraft*, Vol. 37, No. 4, 2000, pp. 580–587.

[12]Schroeder, J. A., Chung, W. W. Y., Tran, D. T., Laforce, S., and Bengford, N. J., "Pilot-Induced Oscillation Prediction with Three Levels of Simulation Motion Displacement," AIAA Paper 98-4333, Aug. 1998.

[13]Chung, W. W. Y., Schroeder, J. A., and Johnson, W. W., "Effects of Vehicle Bandwidth and Visual Spatial-Frequency on Simulation Cueing Synchronization Requirements," AIAA Paper 97-3655, Aug. 1997.

[14]Hess, R. A., and Zeyada, Y., "A Guide to the Use of Multi-loop Pilot/Vehicle Analysis (MPVA)," Dept. of Mechanical and Aeronautical Engineering, Univ. of California, Davis, CA, June 2002.

[15]Heffley, R. K., Jewell, W. F., Lehman, J. M., and Van Winkle, R. A., "A Compilation and Analysis of Helicopter Handling Qualities Data, Vol. One: Data Compilation," NASA CR-3144, March 1979.

[16]Hess, R. A., "Analytical Display Design for Flight Tasks Conducted Under Instrument Meteorological Conditions," *IEEE Transactions on Systems, Man, and Cybernetics*, Vol. SMC-7, No. 6, 1977, pp. 453–462.

[17]Dander, V., "An Evaluation of Four Methods for Converting Single-Axis Pilot Ratings to Multi-Axis Ratings Using Fixed Base Simulation Data," Master's Thesis, Dept. of Electrical Engineering, GE/EE/62-4, U.S. Air Force Inst. of Technology, Wright–Patterson, AFB, OH, Dec. 1962.

[18]McRuer, D., and Schmidt, D. K., "Pilot-Vehicle Analysis of Multiaxis Tasks," *Journal of Guidance, Control, and Dynamics*, Vol. 13, No. 2, 1990, pp. 348–355.

[19]Schroeder, J. A., "Evaluation of Simulation Motion Fidelity Criteria in the Vertical and Directional Axes," *Journal of the American Helicopter Society*, Vol. 41, No. 2, 1996, pp. 44–57.